Kidney International, Vol. 62 (2002), pp. 1933–1946

GENETIC DISORDERS – DEVELOPMENT

Globotriaosylceramide accumulation in the Fabry kidney is cleared from multiple cell types after enzyme replacement therapy

Beth L. Thurberg, Helmut Rennke,[1] Robert B. Colvin,[1] Steven Dikman,[1] Ronald E. Gordon, A. Bernard Collins, Robert J. Desnick, and Michael O'Callaghan

Departments of Pathology and Preclinical Biology, Genzyme Corporation, Cambridge, and Department of Pathology, Brigham and Women's Hospital, and Department of Pathology, Massachusetts General Hospital, Boston, Massachusetts; Departments of Pathology and Human Genetics, Mount Sinai School of Medicine, New York, New York, USA

Globotriaosylceramide accumulation in the Fabry kidney is cleared from multiple cell types after enzyme replacement therapy.

Background. Fabry disease, a lysosomal storage disease caused by deficient lysosomal α-galactosidase A activity, is characterized by globotriaosylceramide (GL-3) accumulation in multiple cell types, particularly the vasculature, leading to end organ failure. Accumulation in the kidney is responsible for progressive decline in renal function in male patients with the classical phenotype, resulting in renal failure in their third to fifth decades of life. With the advent of recombinant protein synthesis technology, enzyme replacement therapy has become a viable alternative to dialysis or renal transplantation, previously the only available treatment options for end-stage renal disease.

Methods. The pre- and post-treatment renal biopsies were analyzed from fifty-eight Fabry patients enrolled in a Phase 3 double-blind, randomized, placebo-controlled trial followed by a six-month open label extension study of the recombinant human enzyme, α-galactosidase A (r-hαGalA), administered IV at 1 mg/kg biweekly. The purpose of this investigation was to detail the pathologic changes in glycosphingolipid distribution and the pattern of post-treatment clearance in the kidney.

Results. Baseline evaluations revealed GL-3 accumulations in nearly all renal cell types including vascular endothelial cells, vascular smooth muscle cells, mesangial cells and interstitial cells, with particularly dense accumulations in podocytes and distal tubular epithelial cells. After 11 months of r-hαGalA treatment there was complete clearance of glycolipid from the endothelium of all vasculature as well as from the mesangial cells of the glomerulus and interstitial cells of the cortex. Moderate clearance was noted from the smooth muscle cells of arterioles and small arteries. Podocytes and distal tubular epithelium also demonstrated evidence for decreased GL-3, although this clearance was more limited than that observed in other cell types. No evidence of immune complex disease was found by immunofluorescence despite circulating anti-r-hαGalA IgG antibodies.

Conclusions. These findings indicate a striking reversal of renal glycosphingolipid accumulation in the vasculature and in other renal cell types, and suggest that long-term treatment with r-hαGalA may halt the progression of pathology and prevent renal failure in patients with Fabry disease.

Fabry disease is an X-linked recessive disorder in which affected males are deficient in the lysosomal enzyme α-galactosidase A. This deficiency leads to accumulation of neutral glycosphingolipids, mainly globotriaosylceramide (GL-3, also referred to as Gb3, ceramide trihexoside, CTH), in tissues throughout the body. Progressive glycosphingolipid accumulation results in clinical disease, primarily in affected males, but some female heterozygotes may be symptomatic depending on the pattern of Lyonization [1–3]. In affected males with the classical phenotype who have absent or very low levels of α-galactosidase A activity, angiokeratomas, hypohidrosis, acroparesthesias, transient ischemic attacks and stroke, congestive heart failure, cardiac conduction abnormalities, myocardial infarction, and progressive renal failure are the major clinical manifestations of the disease [4]. Atypical variants with residual α-galactosidase A have a milder phenotype with manifestations limited to the heart (that is, the cardiac variant [5, 6]). Of note, most cardiac variants do not have endothelial glycosphingolipid deposition, do not develop renal failure and live a normal lifespan, but usually die of the late cardiac manifestations of the disease. In contrast, progressive renal failure in affected males with the "classic" form of Fabry disease limits their average lifespan to the early forties, in the absence of dialysis or renal transplantation [7, 8]. Until the recent advent of recombinant enzyme

[1] Dr. Rennke, Dr. Colvin, and Dr. Dikman contributed equally to this study.

Key words: renal disease, Fabry disease, X-linked recessive disorder, neutral glycosphingolipids, renoprotection, end-stage renal disease, Phase 3 trial.

Received for publication March 22, 2002
and in revised form June 24, 2002
Accepted for publication July 22, 2002

replacement therapy [9], little could be done to combat the underlying pathology of Fabry disease, particularly the progressive renal disease and vascular pathology responsible for the early demise of most patients. Recently, a Phase 1/2 trial [9] and a Phase 3 trial with an open label extension [10] were conducted to evaluate the safety and efficacy of recombinant human α-galactosidase A (r-hαGalA) replacement therapy. These trials demonstrated that r-hαGalA replacement completely cleared GL-3 inclusions from the renal peritubular (interstitial) capillary endothelium (the primary endpoint of the Phase 3 trial) and effected equally remarkable clearance from the capillary endothelium of other key tissues (heart, skin and liver). Clearance of GL-3 from the plasma, urinary sediment and homogenized kidney tissue also was demonstrated. The identity of GL-3 and its clearance from these samples were demonstrated by light microscopic, immunohistochemical and biochemical analyses [9, 10]. The endothelial end points for these Fabry trials were chosen based on evidence implicating underlying vascular injury as the primary cause of the secondary kidney pathology such as global glomerulosclerosis and interstitial fibrosis [11, 12].

Vascular injury has been implicated in organ damage to the skin, heart, liver and CNS [4, 13]. The vascular endothelium plays an important normal physiologic role in glomerular perfusion, filtration, and maintenance of a continuous anti-coagulant vascular lining. Injury to endothelial cells in other disease settings leads to vasoconstriction within the glomerulus, and intravascular inflammation and thrombosis of vessels in the renal cortex and medulla, causing renal injury and failure [14–17] as well as complications such as accelerated atherosclerosis and thromboembolism [18]. More recently, investigators have surveyed Fabry patients and confirmed the elevation of markers of endothelial cell injury and activation [intracellular adhesion molecule-1 (ICAM-1), vascular cell adhesion molecule-1 (VCAM-1), P-selectin], leukocyte activation (CD11b) and coagulation [tissue plasminogen activator (tPA), von Willebrand factor (vWF), plasminogen activator inhibitor (PAI)] [11, 13]. These abnormalities suggest that the vascular endothelial cells of Fabry patients are in a chronic pro-inflammatory and pro-thrombotic state [11, 13]. Loss of nephrons from vascular injury leads to increased pressures on remaining nephrons, leading to further accelerated nephron injury. Clearance of GL-3 from the endothelium by r-hαGalA, therefore, is expected to alleviate ongoing vascular damage and prevent progressive perfusion deficits that would otherwise contribute to renal failure in these patients.

The primary emphasis of the Phase 3 clinical trial was on establishing the significance of the vascular endothelial endpoints and monitoring numerous clinical and safety parameters [10]. A substantial effort also focused on characterizing the pathologic patterns of GL-3 accumulation in the kidneys of these Fabry patients and documenting the response of the various cell and tissue types to r-hαGalA treatment. Although a number of case reports have described the main morphologic characteristics of renal pathology and glycolipid accumulation in renal tissue from Fabry patients [2, 19], little information is available on the patterns of pathology among a larger group of patients and the response of the cell types containing GL-3 to recombinant enzyme therapy. Here, based on a comprehensive analysis of the relevant renal cell types, we report on the clearance characteristics of each cell type in response to r-hαGalA (1 mg/kg biweekly). The pattern of response in the different renal cell types provides insight into treatment strategies that are likely to succeed in improving the overall health of the kidney. The findings are encouraging for the long-term benefits of r-hαGalA replacement therapy in patients with Fabry disease.

METHODS

Patients and study design

The study population comprised 58 Fabry patients (56 males, 2 females) enrolled in a five-month Phase 3, double-blind, randomized, placebo-controlled trial (29 patients in the treatment and placebo arms, mean age ± SD, 28.4 ± 11.4 and 32.0 ± 9.4 years, respectively). This was followed by an additional six-month open label extension study, in which all 58 patients received enzyme replacement therapy. Entry criteria required that patients be 16 years of age or greater, with native plasma α-galactosidase A levels less than 1.5 ng/mL, and baseline serum creatinine levels less than or equal to 2.2 mg/dL. Recombinant α-galactosidase A (r-hαGalA; agalsidase beta; Fabrazyme; Genzyme, Cambridge, MA, USA) at a dose of 1 mg per kilogram of body weight or placebo (phosphate-buffered mannitol) was administered intravenously at a rate of 0.25 mg per minute, every two weeks. Complete sets of three diagnostic quality renal biopsies taken per protocol at baseline, five months and 11 months, were available for 48 of the 58 patients. The remaining ten patient sample sets were available but were limited to one or two of the three time points.

Light microscopy

Preliminary studies revealed that the lipid was best demonstrated for light microscopy in one-micron, epon embedded sections. Therefore, renal biopsies were fixed in 3% glutaraldehyde in 0.2 mol/L sodium cacodylate buffer, pH 7.3, followed by post-fixation in 1% osmium tetroxide in 0.2 mol/L sodium cacodylate (Electron Microscopy Sciences, Fort Washington, PA, USA). The tissue was infiltrated overnight, and then embedded in a 1:1 mixture of Epon 811 A and B (Electron Microscopy Sciences), plus DMP-30/Propylene Oxide (Electron Mi-

croscopy Sciences). One micron sections were stained with a 1:1 mixture of Methylene Blue in 1% sodium borate and 1% Azure II (Fisher Scientific, Fairlawn, NJ, USA).

Scoring of light microscopy

Each renal biopsy was reviewed under light microscopy by three independent renal pathologists who were blinded to treatment status of the patient at the time of biopsy. All pathologists participated in preliminary sessions to establish the criteria for the grading scale used to evaluate baseline GL-3 content and subsequent clearance from affected tissues. Cell types evaluated included: peritubular (interstitial) capillary endothelial cells (the primary endpoint of the Phase 3 trial), glomerular endothelial cells, mesangial cells, arterial/arteriolar endothelial cells, vascular smooth muscle cells, interstitial cells (a mixed cell population of fibroblasts and phagocytic cells), podocytes, and the epithelium of distal convoluted tubules and collecting ducts. The mesangial cell matrix of individual glomeruli was also evaluated for pathologic change. Scoring of these elements was conducted according to the design shown in Table 1. For each cell type listed, a majority score (the score common to at least 2 of the 3 evaluating pathologists) was derived from the individual scores of the three pathologists. When there was no common score for the primary endpoint (peritubular endothelial cells), the pathologists were reconvened for an adjudication. They reviewed the slide together at a multi-headed scope to reach a consensus score. For other cell types, the median score was selected. The distribution of these scores is summarized in Figure 1 and Table 2. Figure 1 shows the distribution of the means of all scores available at each time point. Table 2 shows the distribution of the score shifts from baseline. The differences in the "*N*" values between these two images are due to different presentation of the data. In some instances, certain cell types were absent from individual biopsy samples, and could not be evaluated at all time points. To allow for the variation occurring among glomeruli, the mesangial cell matrix for each individual glomerulus in the biopsy samples (to a maximum of 8) received a score ranging from 0 to 2. Individual glomerular scores were then averaged for each pathologist. The mean for the three pathologists' scores was then calculated.

Electron microscopy

Thin sections were cut from the tissue blocks prepared above and stained with 5% uranyl acetate (in a 1:1 mixture, methanol:water) and a modified Reynold's Lead Citrate. Photographs were taken at ×3300 and ×10,000 magnification using a JEM 100CX electron microscope (JEOL, Ltd, Tokyo, Japan).

Table 1. Scoring system for GL-3 accumulation/clearance in different renal cell types

Cell/tissue	Score
Glomerular endothelial cells Peritubular capillary endothelial cells Arterial/arteriolar endothelial cells Vascular smooth muscle cells Podocytes[a] DCT/collecting ducts[a]	0 = None or trace accumulation 1 = Mild accumulation 2 = Moderate accumulation 3 = Severe accumulation
Mesangial cells: GL-3 accumulation Interstitial cells	0 = No lipid granules 1 = Minimal lipid granules 2 = Numerous lipid granules
Mesangial matrix	0 = Normal mesangium 1 = Mild expansion 2 = Moderate expansion

[a] For the podocytes and distal convoluted tubules (DCT)/collecting ducts, an increase (+), a decrease (−) or no change (0) response was collected for all post-baseline scores by comparing the baseline biopsy to a 5 or 11 month biopsy. Therefore, there are no absolute baseline values for these cell types, only relative values at 5 months and 11 months that reflect a comparison to the baseline.

Immunofluorescence

Immunofluorescence studies also were performed to determine whether IgG antibodies against r-hαGalA, which developed in most patients receiving the enzyme, had resulted in immune complex deposition in the kidney. Frozen tissue samples from five r-hαGalA-treated patients who developed IgG antibodies by the five month biopsy (IgG+ Group), three r-hαGalA–treated patients who did not develop IgG antibodies at five months (IgG− Group), and five untreated placebo patients (Control Group) were analyzed. Pre-treatment, baseline samples were available from two of these patients (one IgG+ and one IgG−). Four-micron sections from fresh frozen blocks of renal biopsies were stained with IgG fractions of fluorescein-conjugated monospecific antisera to human IgG, IgA, IgM, C3, C1q, fibrin/fibrinogen, and albumin (Dako Corp., Carpinteria, CA, USA) by standard clinical techniques [20]. Frozen sections were cut in a cryostat at −20°C and placed on Fisher Superfrost Plus slides (Fisher Scientific) and then air-dried. Using a Tissue-Tek II slide staining unit, slides were placed on a clinical rotator and pre-washed for five minutes in 0.01 mol/L sodium-phosphate-buffered saline (PBS), 0.15 mol/L NaCl, pH 7.3. One drop (50 to 100 μL) of diluted fluorescein conjugate was applied to the tissue section. The optimal concentration for each conjugate was determined by titering on known positive and negative control tissues. Slides were then incubated in a moist, level, covered chamber for 30 minutes at room temperature. After incubation, the slides were washed in PBS for five minutes × 4. The excess PBS was blotted from around the specimen, and the moistened tissue was coverslipped with Aquamount

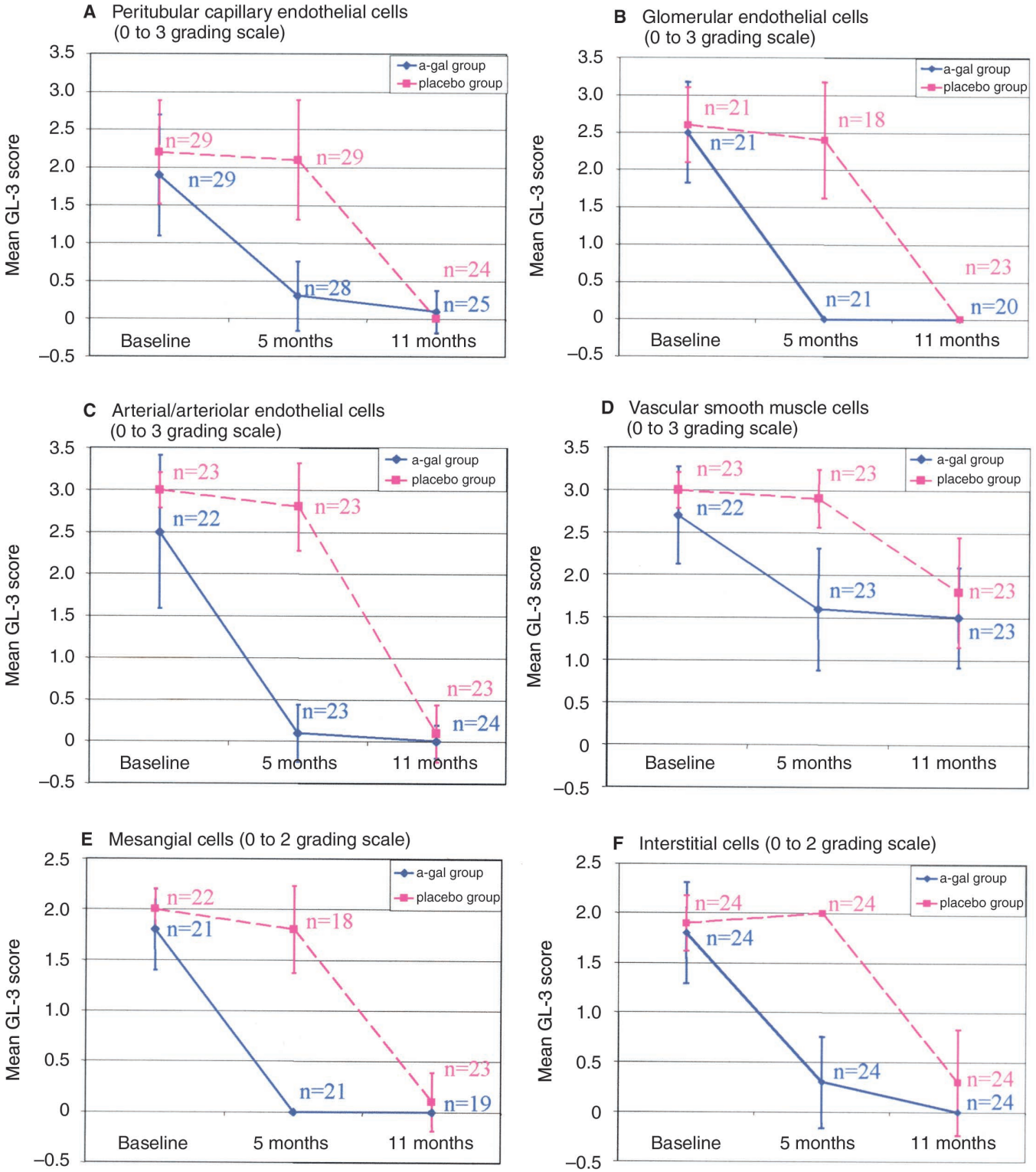

Fig. 1. Mean globotriaosylceramide (GL-3) scores with standard deviations were calculated for each cell type above in both the treatment groups at baseline, 5 months and 11 months. Note the rapid decline in mean GL-3 scores for the placebo group once enzyme replacement therapy was initiated after the 5-month time point. Treatment groups maintained their low GL-3 scores from the pivotal study (baseline to 5 months) into the extension segment of the study (evaluated at 11 months). (*A*) Peritubular capillary endothelial cells; (*B*) glomerular capillary endothelial cells; (*C*) arterial/arteriolar endothelial cells; (*D*) vascular smooth muscle cells; (*E*) mesangial cells; (*F*) interstitial cells. (Note: The differences in the "*N*" values between Figure 1 and Table 2 are due to different presentation of the data. In some instances, certain cell types were absent from individual biopsy samples, and could not be evaluated at all time points. Hence, the shift data presented in Table 2 have lower "*N*" values in some cases.)

Table 2A. Percentage of patients achieving zero scores*
(percentages of patients with a 1–3 point score reduction, including all zero scores, are shown in parentheses)

		Score shift from baseline to 5 months			Score shift from baseline to 11 months		
Renal cells evaluated	TX group	Baseline	5 months	*N*	Baseline	11 months[a]	*N*
Peritubular capillary endothelial cells	Placebo	0%	0% (38%)	29	0%	100% (100%)	24
	A-gal	3%	69% (86%)	29	0%	92% (96%)	25
Glomerular capillary endothelial cells	Placebo	0%	0% (31%)	16	0%	100% (100%)	21
	A-gal	0%	100% (100%)	19	0%	100% (100%)	17
Mesangial cells	Placebo	0%	0% (19%)	16	0%	90% (100%)	21
	A-gal	0%	100% (100%)	19	0%	100% (100%)	17
Interstitial cells	Placebo	0%	0% (0%)	24	0%	78% (91%)	24
	A-gal	4%	71% (100%)	24	4%	100% (100%)	24
Arterial/arteriolar endothelial cells	Placebo	0%	0% (19%)	22	0%	87% (100%)	22
	A-gal	10%	86% (100%)	21	9%	96% (100%)	22
Vascular smooth muscle cells	Placebo	0%	0% (10%)	22	0%	0% (86%)	22
	A-gal	0%	10% (86%)	21	0%	0% (81%)	21

*The clearance of GL-3 from multiple renal cell types was determined before and after enzyme replacement therapy. There were two groups of patients: (*1*) the placebo group received placebo for the first 5 months and then α-galactosidase A for the remaining 6 months and (*2*) the A-gal group which received α-galactosidase A for the entire 11 months. The percentage of patients who attained a zero score at each biopsy time point is displayed and the percentage of all patients who demonstrated a reduction in score, including all zeros, is in parentheses. Values are presented for both the placebo and treatment groups. For statistical purposes, it was necessary for each patient to have both a baseline score and a shift score (5 months or 11 months) for each cell type, in order to be included in this data set. Two baseline columns are presented; the "*N*" designates the number of paired scores available for each cell type (paired scores meaning baseline and 5 months, or baseline and 11 months). This permitted calculation of the statistical significance of the change in score from either baseline to 5 months, or from baseline to 11 months, when comparing the placebo and treated groups. This distinction was necessary because (*1*) some patients had a poorly preserved or missed biopsy at one of the time points, and (*2*) some biopsy specimens did not contain glomeruli and therefore those cells could not be evaluated at all time points.

Table 2B. Percentage of patients achieving a reduction in GL-3 relative to baseline*

		5 months		11 months[a]	
	TX group	%	*N*	%	*N*
Tubular epithelium	Placebo	4%	24	78%	24
	A-gal	25%	24	50%	24
Podocytes	Placebo	0%	16	23%	22
	A-gal	5%	19	18%	17

*Tubular epithelium and podocyte clearance were expressed as the percentage of patients attaining a relative reduction in the 5 month and 11 month biopsy. An increase (+), a decrease (−) or no change (0) response was collected for all post baseline scores by comparing the baseline biopsy to a 5 or 11 month biopsy. Therefore, there are no absolute baseline values for these cell types, only relative values at 5 months and 11 months that reflect a comparison to the baseline. A-gal represents patients treated with the recombinant human enzyme, α-galactosidase A.

[a]Placebo group has crossed over to treatment at this time point

and glycerol (Lerner Labs, Pittsburgh, PA, USA). Coded slides were scored blinded, without knowledge of treatment groups or antibody status, using an epi-illumination fluorescence microscope. The intensity and distribution of glomerular staining was scored from 0 to 4 for each of the antibodies.

RESULTS

Baseline biopsies

At baseline, GL-3 accumulation in the kidney tissues was extensive, but varied considerably in quantity and morphology among the different cell types (Fig. 2). Podocytes and distal tubular epithelial cells contained the highest concentrations of GL-3 inclusions, whereas proximal tubular epithelial cells were relatively unaffected. The appearance of the lipid inclusions also varied, appearing in some cell types as small, dark, dense beaded granules, and in others as larger, complex, laminated bodies (myelin figures).

Globotriaosylceramide accumulation in vascular endothelial cells appeared as small, dense, beaded, perinuclear cytoplasmic inclusions. GL-3 also accumulated in severely affected cells as larger grouped inclusions in the peripheral cytoplasm. The larger cytoplasmic inclusions often clustered and protruded into the lumens of small capillaries (Figs. 3A and 4A). On electron microscopy many of these granules were dense and amorphous (Fig. 3C). Vascular smooth muscle cells also accumulated moderate amounts of granular, cytoplasmic GL-3 (Fig. 5A). GL-3 in mesangial cells appeared as dense granules clustered around the nucleus in the cytoplasm (Fig. 6A). Interstitial fibroblasts and phagocytic cells ("interstitial cells") of the renal cortex also shared a similar appearance (Fig. 7A).

Lipid accumulation in podocytes and the epithelial cells of distal convoluted tubules and collecting ducts was much more concentrated and extensive than the accumulation present in endothelial cells, smooth muscle cells, mesangial cells or interstitial cells. Podocyte nuclei were often eccentrically positioned, pushed aside by the mass of accumulated GL-3 inclusions in the form of multiple scroll-like myelin figures filling the entire cytoplasm (Fig. 8A). The laminated appearance was particularly promi-

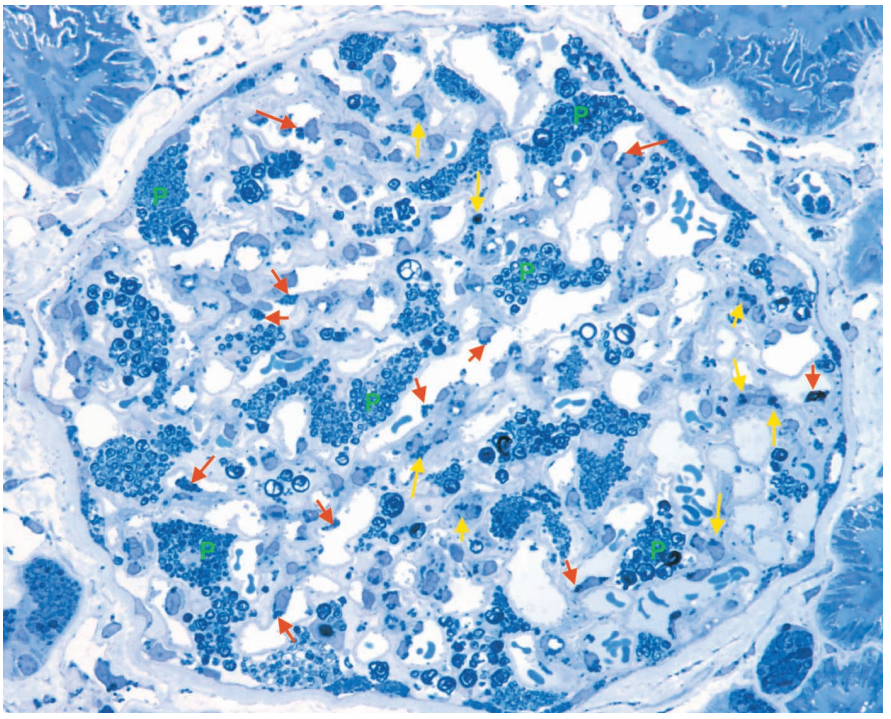

Fig. 2. GL-3 accumulates as dark blue granules and scroll-like whorls in multiple cell types of the renal glomerulus. Red arrows indicate endothelial accumulation; yellow arrows indicate mesangial cell accumulation; green "P" indicates podocyte accumulation (Magnification, ×40 objective).

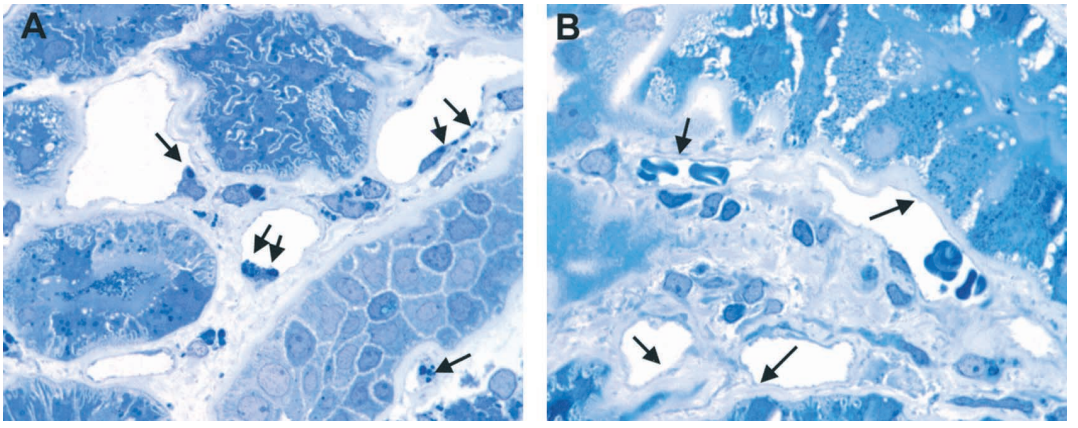

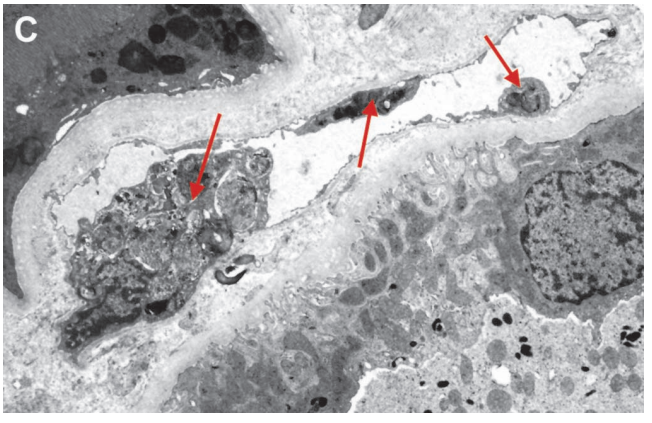

Fig. 3. GL-3 is cleared from endothelial cells of the peritubular (interstitial) capillaries. (*A*) Baseline biopsy, pre-treatment. GL-3 is present near endothelial nuclei and around the perimeter of the capillaries. (*B*) Post-treatment biopsy. Capillaries are clear of GL-3 (magnification of A and B, ×100 objective). (*C*) Electron microscopic image of capillary endothelial cell GL-3 accumulations (arrows) protruding into the lumen, at baseline (Magnification, ×3300).

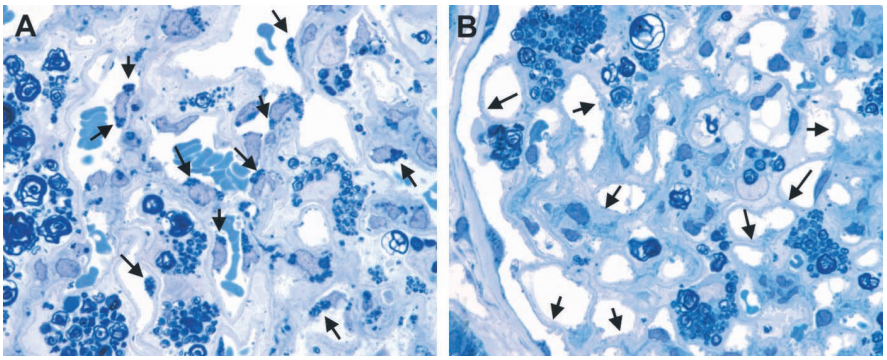

Fig. 4. GL-3 is cleared from endothelial cells of the glomerular capillaries. (*A*) Baseline biopsy, pre-treatment. Note how large clusters of GL-3 granules protrude into the vascular lumens of the glomerular capillaries. (*B*) Post-treatment biopsy. Protruding GL-3 clusters have been completely removed from the glomerular capillary lumens (magnification, ×100 objective).

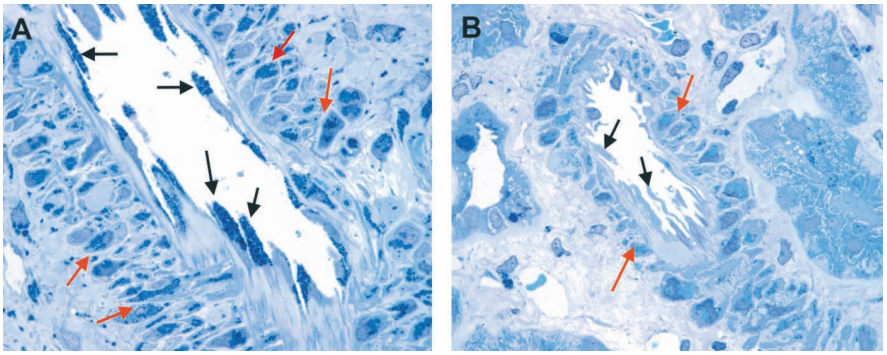

Fig. 5. GL-3 is cleared from endothelial cells (black arrows) and smooth muscle cells (red arrows) of renal arterioles. (*A*) Baseline biopsy, pre-treatment. Note how GL-3 accumulates in very large clusters in endothelial cells of these larger vessels. (*B*) Post-treatment biopsy. Both endothelial cells and smooth muscle cells of this vessel have achieved significant clearance of GL-3 (magnification, ×100 objective).

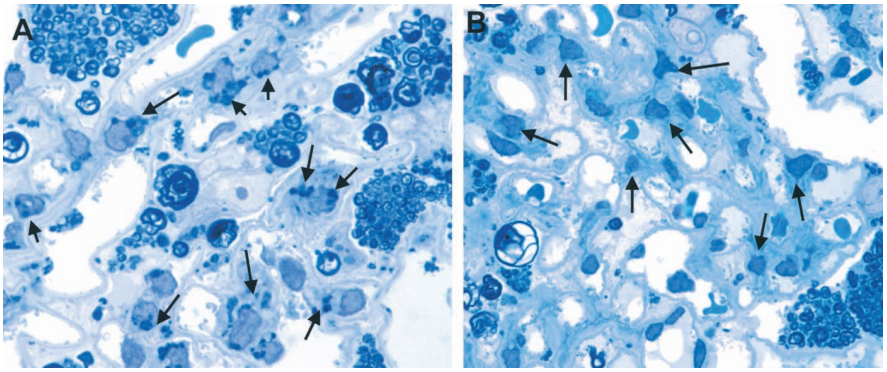

Fig. 6. GL-3 is cleared from mesangial cells. (*A*) Baseline biopsy, pre-treatment. Dense GL-3 granules accumulate around the nuclei of mesangial cells. (*B*) Post-treatment. Mesangial cells are completely cleared of GL-3 (magnification, ×100 objective).

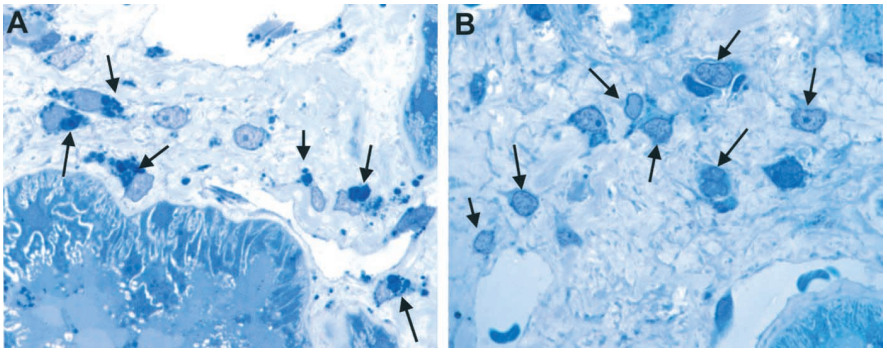

Fig. 7. GL-3 is cleared from interstitial cells. (*A*) Baseline biopsy, pre-treatment. GL-3 fills most of the cytoplasm of these interstitial cells. (*B*) Post-treatment. The interstitial cell cytoplasm has been cleared of GL-3 (magnification, ×100 objective).

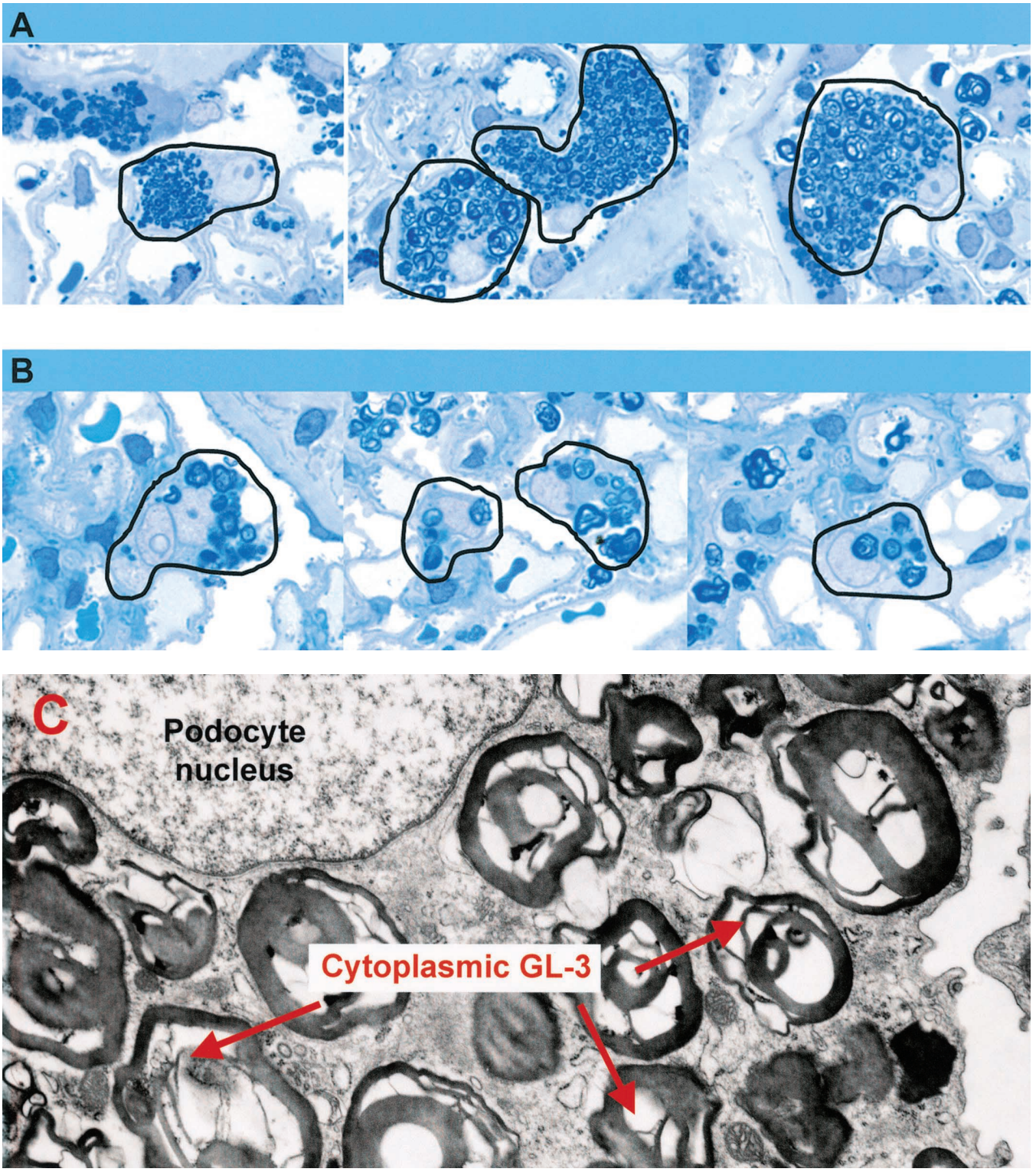

Fig. 8. GL-3 is cleared from podocytes. (*A*) Baseline biopsy, pre-treatment. GL-3 appears as multiple, tight scroll-like figures that fill the cytoplasm of each podocyte. (*B*) Post-treatment. The scroll-like GL-3 forms are looser and less numerous after treatment. Podocytes are outlined pre- and post-treatment for emphasis (magnification of A and B, ×100 objective). (*C*) Electron microscopic image demonstrating the lamellar ultrastructure of the GL-3 accumulation in podocyte cytoplasm at baseline (magnification, ×10,000).

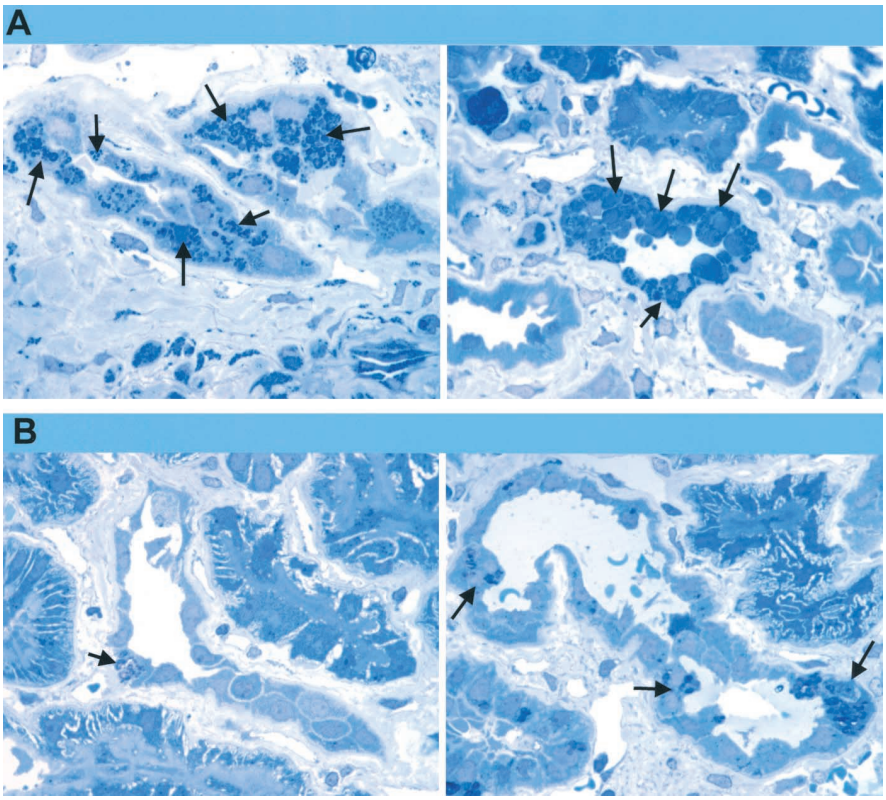

Fig. 9. GL-3 is cleared from tubular epithelium. (*A*) Baseline biopsy, pre-treatment. GL-3 appears as multiple small and large dense granules, some with a scroll-like architecture, within the epithelial cell cytoplasm of distal convoluted tubules and collecting ducts. (*B*) Post-treatment. The granules are fewer in number after treatment (magnification, ×100 objective).

nent by electron microscopy (Fig. 8C). GL-3 accumulations in the epithelium of distal convoluted tubules and collecting ducts were similar in concentration and appearance to those in the podocytes (Fig. 9A).

Post-treatment biopsies

Vascular endothelium. Treatment with r-hαGalA resulted in statistically significant clearance of lipid from endothelial cells of all vessel types examined: peritubular capillaries, glomerular capillaries and arterial/arteriolar vessels.

In the patient group receiving r-hαGalA from baseline to five months, 86% demonstrated a reduction (or maintained a zero score) in GL-3 from peritubular capillary endothelial cells (Fig. 3B); 69% of patients achieved an endothelial score of zero (baseline mean = 1.9; five-month post-treatment mean = 0.3; Fig. 1A). After an additional six months of treatment, 96% of patients in this treatment group demonstrated a reduction in score (relative to baseline), with 92% achieving a score of zero (complete clearance), as demonstrated by biopsy at month 11. In the placebo group, 38% of patients demonstrated a reduction in GL-3 from baseline to five months; however, none (0%) achieved a score of zero (baseline mean = 2.2; five-month post-placebo mean = 2.1; Fig. 1A). There was a statistically significant difference between r-hαGalA and placebo-treated patients in the placebo-controlled (5 month) study ($P < 0.001$; based on a χ^2 test). After crossover to treatment for an additional six months, 100% (Table 2A) of the former placebo patients achieved an endothelial score of zero at month 11, demonstrating complete clearance ($P < 0.001$).

For glomerular capillary endothelial cells, patients receiving r-hαGalA from baseline to five months demonstrated 100% clearance of GL-3 (Fig. 4B), all attaining endothelial scores of zero (baseline mean = 2.5; five-month post-treatment mean = 0.0; Fig. 1B). All patients in this treatment group maintained a score of zero (complete clearance) after an additional six months of treatment. In the placebo group, 0% of patients attained zero endothelial scores from baseline to five months (baseline mean = 2.6; five-month post-placebo mean = 2.4; Fig. 1B). There was a statistically significant difference between the r-hαGalA and placebo treated patients in the placebo-controlled (5 month) study ($P < 0.001$). After crossover to treatment for an additional six months, however, 100% of the former placebo patients achieved endothelial scores of zero at month 11, demonstrating complete clearance ($P < 0.001$).

Examination of the arterial/arteriolar endothelial cells demonstrated that 100% of the rh-αGalA–treated patients had reduced GL-3 levels (Fig. 5B), with 86% achieving a score of zero from baseline to five months (baseline mean = 2.5; five-month post-treatment mean = 0.1; Fig.

1C). After an additional six months of treatment, these patients continued to improve, with 96% achieving a score of zero for complete clearance. In the placebo group, 19% of patients demonstrated a reduction in GL-3 score, however, none received a score of zero from baseline to five months (baseline mean = 3.0; five-month post-placebo mean = 2.8; Fig. 1C). There was a statistically significant difference in the percentage of zero scores between treated and placebo groups in the placebo-controlled study ($P < 0.001$). After the crossover to enzyme therapy for six months, 100% of the former placebo patients demonstrated a reduction in GL-3 score with 87% achieving zero scores ($P < 0.001$; Table 2A).

Vascular smooth muscle cells. Enzyme therapy removed GL-3 from vascular smooth muscle cells (Fig. 5B), although the clearance was less complete than that observed in other cell types. In the patient group treated with r-hαGalA from baseline to five months, 86% demonstrated a reduction in GL-3 score; however, only 10% received zero scores (baseline mean = 2.7; five-month post-treatment mean = 1.6; Fig. 1D). After an additional six months of treatment these values were relatively unchanged, as 81% demonstrated a reduction in GL-3 score and 0% had a score of zero. At this time point, reversal of zero scores occurred in two patients: one received a score of 1 and the other received a score of 2. In the placebo group, 10% of patients demonstrated a reduction in GL-3 score, however, none achieved a score of zero (baseline mean = 3.0; five-month post-placebo mean = 2.9; Fig. 1D). After crossover to treatment with r-hαGalA for an additional six months, 86% (Table 2A) demonstrated a reduction in GL-3 score and the mean score declined to 1.8 (Fig. 1D).

Mesangial cells. The lipid inclusions in mesangial cells of the renal glomeruli were cleared after five months of enzyme treatment (Fig. 6B). Scored on a scale from 0 to 2, the mesangial cells of all patients (100%) treated with rh-αGalA from baseline to five months demonstrated complete clearance (zero scores) of GL-3, and maintained their zero scores after an additional six months of r-hαGalA (baseline mean = 1.8; 5 and 11 month post-treatment means = 0.0; Fig. 1E). In the placebo group, 19% of patients showed a reduction in GL-3 scores, however, none achieved a score of zero from baseline to five months (baseline mean = 2.0; five month post-placebo mean = 1.8; Fig. 1E). There was a statistically significant difference in the percentage of zero scores between treated and placebo patients during the placebo-controlled study ($P < 0.001$). After crossover to treatment for an additional six months, 100% of the former placebo patients achieved a reduction in GL-3, with 90% (Table 2A) receiving a zero score indicating complete clearance of glycosphingolipid from the mesangial cells ($P < 0.001$).

Mesangial cell matrix. At baseline, both treatment groups had moderate mesangial matrix widening (r-hαGalA–treated group, mean score = 0.8; placebo group, mean score = 0.9). There was no statistically significant difference between the mean scores from baseline to five months for the amount of matrix in either treatment group ($P = 0.284$). Change from baseline to 11 months showed a mean score decrease of only 0.1 for patients treated with the enzyme for the entire 11 months.

Interstitial cells. The lipid in interstitial cells was cleared after five months of treatment in the majority of patients (Fig. 7B). In the r-hαGalA cohort from baseline to five months, 100% demonstrated a reduction (or maintained zero scores) in GL-3 score, with 71% achieving complete clearance of interstitial cell GL-3 (baseline mean = 1.8; five-month post-treatment mean = 0.3; Fig. 1F). After an additional six months of treatment, 100% of the treatment group had achieved zero scores. In the placebo group, 0% achieved zero scores from baseline to five months (baseline mean = 1.9; five month post-placebo mean = 2.0; Fig. 1F). There was a statistically significant difference in the percentage of zero scores between treated and placebo patients in the placebo-controlled study ($P < 0.001$). After crossover to treatment for six months, 91% of the former placebo group demonstrated a reduction in GL-3 score, with 78% (Table 2A) achieving a score of zero ($P < 0.001$).

Epithelial cells: Podocytes and tubular epithelium. Podocytes responded to r-hαGalA enzyme therapy with a modest reduction in the numbers of lamellar GL-3 inclusions (Table 2B), and in many cases a more varied cytoplasmic GL-3 morphology, with some myelin figures being reduced to loose scroll-shaped bodies floating in the cell cytoplasm (Fig. 8B). In the r-hαGalA treated group, 5% showed a reduction in podocyte GL-3 after five months. This increased to 18% after an additional six months of treatment, demonstrating continued improvement of GL-3 clearance. In the placebo group, 0% of patients showed a reduction in GL-3 accumulation from baseline to five months. After crossover to treatment for an additional six months, 23% of patients began to show a relative reduction in podocyte GL-3 (Table 2B).

For the tubular epithelium, 25% of the samples in the r-hαGalA-treated group from baseline to five months demonstrated a relative reduction in GL-3 accumulation. After an additional six months of treatment in the extension study, 50% of these patients demonstrated a reduction in GL-3 (Fig. 9B). In the placebo group, only 4% demonstrated a reduction in GL-3 from baseline to five months; however, after crossover to r-hαGalA treatment for an additional six months, 78% of patients in this group demonstrated a relative reduction in tubular epithelium GL-3 (Table 2B).

Immunofluorescence for immune complex deposition. None of the patient samples tested (5 anti-r-hαGalA IgG positive, 3 anti-r-hαGalA IgG negative, 5 placebo, and

Table 3. Immunofluorescence result on glomerular deposits

Biopsy #	IgG anti-rhαGAL	IgG		IgA		IgM		C3		C1q		Fibrin/fibrogen	
		GBM	Mes	GBM	Mes	GBM	Mes	GBM	Mes	GBM	Mes	GBM	Mes
Treated, with IgG titers	titer												
349	25600	0	0	0	0	0	0.5	0	0.5	0	0	0	0
359	25600	0.5	0	0.5	0.5	2	0.5	3	1	0	0.5	2	0
463	12800	0	0	0	0	0	0.5	0	0.5	0	0	0	0
73	12800	0	0	0	0	0	0.5	0	0.5	0	0	0	0
207	12800–25600	0	0	2	1	2	0.5	0	0.5	0	0	0	0.5
207 Pre	pre-treatment	0	0	0.5	1	2	1	0	0.5	0	0	0	0.5
Placebo with no IgG titers													
323		0	0	0.5	0.5	0	0.5	0	0.5	0	0	2	0.5
118		0	0	0	0	0	0.5	0	0.5	0	0	0.5	0.5
127		0	0	0.5	0.5	0	0.5	0	0.5	0	0	0.5	0.5
103		0	0	0	0	3	0.5	0	0.5	0	0	0.5	0.5
289		0	0	0	0	2	1	0	0.5	0	0	0	0.5
Treated, no IgG titers													
232		0	0	0	0	0.5	0.5	0.5	0.5	0	0	0	0
52		0	0	0	0	0.5	1	0	0.5	0	0	0.5	0.5
23		0	0	2	2	0.5	0	0.5	0.5	0	0	2	0.5
23 Pre	pre-treatment	0	0	1	2	2	1	0	0	0	0	0	0.5

Summary table of immunofluorescence results on immune complex deposition in the glomeruli of Fabry patients on Fabrazyme. Abbreviations are: GBM, glomerular basement membrane; Mes, mesangium. The intensity and distribution of glomerular staining were scored from 0 to 4 for each of the parameters listed. Note that IgG staining was negligible in all specimens examined for immune complex disease.

2 pre-treatment samples) had more than trace deposits of IgG in their glomeruli detected by immunofluorescence (Table 3). Two patients had IgA deposition, suggestive of IgA nephropathy (one in the IgG positive group and one in the IgG negative group). Pre-treatment samples were available for each of these patients and showed pre-existing IgA deposits. Three others had segmental IgM deposits typical of focal sclerosis (one IgG positive and two IgG negative patients). These findings indicate that despite five months of r-hαGalA treatment, patients with plasma IgG antibodies against the enzyme had no evidence of immune complex deposition in their kidneys.

DISCUSSION

The quantity of GL-3 that accumulates in different cell types in Fabry disease varies considerably. Some cells such as keratinocytes, proximal tubular epithelium and liver parenchyma are relatively devoid of lysosomal inclusions, whereas cardiomyocytes, podocytes and distal tubular epithelial cells are heavily laden. This cell-to-cell variation also is reflected in the total glycolipid content of different organs, in which certain cell types dominate. In the Phase I/II trial, mean whole tissue concentrations of GL-3 were 21,400 ng/mg in the heart, 5530 ng/mg in the kidney, 350 ng/mg in the skin and 1948 ng/mg in the liver [9]. The extremely high level in the heart reflects the predominance of the heavily laden cardiomyocytes in heart tissue, whereas the relatively low level in the liver reflects the dominance of parenchymal cells that were relatively free of GL-3. The kidney falls in the intermediate range since heavily laden cells such as podocytes and distal tubular epithelium are mixed with cell types, such as endothelial cells, containing smaller glycolipid inclusions.

Variation in the amount of accumulated GL-3 among cells deficient in r-hαGalA is presumably determined by the amount of substrate generated by the cell type in question and the rate of cell turnover. The rate at which substrate is cleared will be determined by these same factors, plus the degree of exposure of the cell to the administered replacement enzyme. The ability of the enzyme to pass through various cellular and acellular barriers, such as the glomerular filtration apparatus, will determine its effectiveness at clearing substrate in different cell types. Fabrazyme (r-hαGalA) is a 110 kD dimeric glycoprotein containing mannose-6-phosphate terminated carbohydrates. It has been designed to target the cation-independent mannose-6-phosphate receptor (CIMPR), a receptor present on all normal mammalian cells. The CIMPR cycles continuously from the cell surface where it binds and endocytoses mannose-6-phosphate-containing ligands (such as newly synthesized lysosomal enzymes that have escaped sorting in the Golgi) to the lysosome, where these ligands are released [21, 22].

Of the renal cell types examined in this study, endothelial cells turn over the most frequently [23, 24] and, as demonstrated for the three vessel types examined (peritubular capillaries, glomerular capillaries, and arterioles and small arteries), were cleared of GL-3 within five months of initiating enzyme replacement treatment. Furthermore, as a consequence of intravenous delivery, the mannose-6-phosphate receptors on the surface of endothelial cells are likely to be exposed to the highest concentration of delivered enzyme. Thus, during the limited

50 to 100 day lifespan of endothelial cells [23], only a modest amount of GL-3 accumulates before the cell is replaced. The combination of rapid cell turnover and maximum exposure to r-hαGalA most likely explains the high degree of success in removing GL-3 from this key tissue within the first five months of treatment.

Mesangial cells also have a relatively rapid turnover rate [23] and demonstrated near complete GL-3 clearance within five months of initiating enzyme replacement therapy. The path of exposure of mesangial cells to r-hαGalA is unclear since the glomerular filtration barrier normally traps molecules greater that 69 kD. However, since the mesangial cells are in the immediate plasma filtration pathway of injured glomerular endothelium, which may allow passage of protein, mesangial cells are likely to have relatively high exposure to the enzyme. Immunohistochemical detection of the CIMPR on Fabry renal tissue has demonstrated that mesangial cells, as well as other affected renal cells, are rich in the receptor (Genzyme; unpublished observations). The interstitial cells accumulated small, dense GL-3 granules similar to those seen in endothelial and mesangial cells, and responded to enzyme replacement therapy to a similar degree. The interstitial cell population is comprised of fibroblast-like and phagocytic cells dispersed throughout the extra-glomerular interstitium. While there is little information on the turnover rate of this cell population, the rapid clearance of GL-3 observed suggests that regular cell turnover may play a role in the response of these cells.

The parietal epithelial cells (Bowman's capsule), followed by the visceral epithelial cells (podocytes) have the slowest turnover rate of the renal cell populations [23–25]. The tubular epithelium, however, is regularly shed in the urine and replaced, and has been shown to have a relatively high proliferation index [24]. This may account for the faster rate of GL-3 clearance following initiation of enzyme replacement therapy compared to that of podocytes. However, despite its high proliferation index, the tubular epithelium is more heavily laden with GL-3 than one might at first expect for a cell population that is regularly shed. Reports on the re-accumulation of GL-3 in normal kidneys transplanted into Fabry patients provide some insight into this apparent contradiction. One autopsy case reports the recurrence of Fabry disease in a transplanted kidney 11 years after transplant. Examination of the renal allograft revealed isolated accumulation of GL-3 in the endothelial cells of the capillaries [26]. It was suggested that high circulating levels of plasma GL-3 may overwhelm the enzymatic capacity of endothelial cells, which may accumulate GL-3 from the plasma by passive or endocytotic mechanisms. More importantly, a second autopsy case reported accumulation of GL-3 in both capillary endothelial cells and tubular epithelial cells in a renal allograft 14 years after transplant [27]. Urine is concentrated along the distal convoluted tubules and collecting ducts. Therefore, it is probable that the epithelia of the distal convoluted tubules and collecting ducts are exposed to high concentrations of GL-3, leading to active or passive uptake. This may explain the marked accumulation of GL-3 observed in both this transplanted kidney and in the kidneys of all Fabry patients.

The similarities in the pattern and appearance of GL-3 accumulation in glomerular and tubular epithelia, despite their widely differing functions, are most likely a reflection of their common embryonic origin. The large quantity and organized ultrastructure of GL-3 in highly laminated myelin bodies in podocytes also is consistent with a lifetime of GL-3 accumulation due to untreated disease. Indeed, GL-3 accumulation has been observed in the renal epithelial cells of second trimester, hemizygous fetuses [28, 29], indicating early and active accumulation in these cells. Similar high concentrations of large, highly structured lysosomal inclusions are seen in cardiomyocytes, cells that are terminally differentiated with no regenerative capacity [30]. Given the large quantity of GL-3 in the renal epithelial cells, it is likely that implementation of enzyme replacement therapy over an extended period will be required to effect complete clearance. Since these cells are further down the filtration pathway they may suffer from less exposure to intravenously delivered enzyme. Nonetheless, there was good evidence from histologic examination of the podocytes and distal tubular epithelial cells that r-hαGalA had reduced the high baseline levels of GL-3 in these cells.

Numerous case reports suggest that while damage to podocytes, which play a role in the filtration of plasma proteins, may explain the presence of proteinuria in both hemizygotes and heterozygotes, this aspect alone cannot account for the precipitous renal failure in hemizygous male patients. Although the accumulation of GL-3 in podocytes of Fabry patients is dramatic, the renal pathology of some asymptomatic heterozygous females is often limited to significant accumulations of GL-3 in the podocytes with little alteration in renal function [1–3, 31]. One case report describes the inadvertent use of a heterozygous Fabry donor for transplantation to a genetically normal recipient. The graft was later found to contain numerous epithelial cell inclusions, but continued to function normally for 20 years [32, 33]. There is also a report of a 28-year-old male hemizygote with a subclinical variant of Fabry disease whose only renal pathology was podocyte accumulation of GL-3 [34]. This patient had a partial deficiency of α-galactosidase A. This finding suggests that while his enzyme level was not sufficient to prevent podocyte accumulation, it was enough to prevent clinical disease as seen in female heterozygotes. These cases and others [19, 35–39] suggest that residual enzyme activity, while perhaps not eliminating all signs of clinical or histologic disease, is still able to

significantly extend the patient's lifespan by obviating renal failure.

Most of the patients in the Genzyme-sponsored Phase III trial developed circulating IgG antibodies to r-hαGalA by the 3rd to 7th dose of enzyme [10]. However, the efficacy of r-hαGalA was not impaired by antibody development. This determination is based on the continued reduction in histologic scores for cellular clearance of GL-3 through the Extension study, even in patients who developed transiently higher titers [10]. As a safety measure, we also sought evidence of immune complex deposition in the kidney by immunofluorescence. Despite antibody titers of ≥12,800 units in the five r-hαGalA-treated patients tested, no IgG deposits were found in their glomeruli. Segmental IgM was occasionally present, as expected in lesions with segmental scars, and was not correlated with anti-r-hαGalA antibodies. IgA deposition was detected in two treated patients (one with anti-r-hαGalA antibodies and one without). Similar IgA deposits were present in the pre-treatment biopsies of each patient, indicating that the process pre-dated r-hαGalA exposure.

Recent evidence that the endothelium of Fabry patients is in a pro-inflammatory and pro-thrombotic state [11, 13] supports the predominant role of vascular pathology in the pathogenesis of Fabry disease, including kidney failure [18]. Further evidence for the primary importance of the endothelial cells in the pathophysiology of Fabry disease comes from a comparison of the cardiac variant of Fabry disease with the classical form. Cardiac variant patients have marked GL-3 accumulation in cardiomyocytes, renal tubular epithelium and podocytes, as is seen also in classical Fabry patients, yet cardiac variants demonstrate little to no endothelial accumulation of GL-3. This difference suggests that the extended lifespan enjoyed by cardiac variant patients (relative to the shortened lifespan of classical Fabry patients) may be due to their lack of endothelial GL-3 accumulation. Male cardiac variants have residual enzyme activity, and this may be sufficient to keep endothelial cells clear of GL-3, thereby delaying the renal disease usually responsible for the death of the classical Fabry patient. The extended lifespan of the cardiac variant patient provides time for the GL-3 accumulation in the heart muscle to manifest itself clinically, as these patients often die later in life of cardiac disease [40]. Published case reports illustrate these points. The autopsy of a 63-year-old cardiac variant who died of conduction system abnormalities caused by glycosphingolipid accumulation, also was found to have GL-3 restricted to renal epithelial cells [41]. Clinically, the patient's renal decline was likely delayed by the residual enzyme activity. The absence of vascular endothelial cell involvement has been observed in other cardiac variants as well [42]. These cases suggest that it is not necessary to eliminate all signs of histologic disease to achieve significant clinical benefit by enzyme replacement therapy. As mentioned earlier, complete clearance of a lifetime accumulation of GL-3 from some cell populations, such as cardiomyocytes and podocytes, is likely to require an extended treatment period. The most benefit would be afforded to those who begin treatment early in life, with the aim of arresting GL-3 cellular accumulation at sub-clinical levels. Residual enzyme activity in the cases described appears to maintain clearance of GL-3 from vascular endothelial cells and prevents the thrombosis-related injuries contributing to early morbidity and premature mortality in classical Fabry patients.

Clearance of GL-3 accumulation from cell types other than the vascular endothelium is likely to have considerable benefit for the overall health of the kidney by complementing the anti-inflammatory and anti-thrombotic benefits of vascular endothelial clearance. The mesangium, composed of cells and matrix, provides support to the glomerular capillary tuft. Mesangial cells have contractile properties that mediate filtration, and phagocytic properties that clean debris from the mesangium. Injury to mesangial cells primarily from intracellular GL-3 accumulation, and secondarily from capillary tuft vascular impairment, leads to the proliferation of cells and matrix, which in turn contributes to glomerulosclerosis [11]. During this study, we observed complete removal of GL-3 from mesangial cells and no change in mesangial cell matrix deposition. This observation may indicate either that treated mesangial cells cease or stabilize in their secretion of matrix, or that the deposition of matrix in Fabry disease is too slow to observe appreciable changes during an 11-month period.

The long-term treatment goal for Fabry patients is ultimately to prevent significant kidney pathology from developing by providing enzyme replacement therapy early in life. For older patients, the goal is to halt the progression of existing kidney pathology before the threshold of renal reserve is reached and life-threatening renal failure ensues. Given the effectiveness of r-hαGalA in clearing GL-3 from all of the relevant cell types of the kidney, even if slowly in podocytes and distal tubular epithelial cells, slowing the progression of disease in patients with early signs of renal failure also may be realistic. This pathology study has demonstrated that enzyme therapy with r-hαGalA resulted in significant clearance of the accumulated substrate from not only the critical endothelial compartment, but from all of the cell types involved in the renal pathology of Fabry disease, thereby providing a realistic means of stabilizing the disease and avoiding progression to clinical failure.

ACKNOWLEDGMENTS

This work was supported in part by grants from the National Institutes of Health including a research grant (R29 DK 34045 Merit Award), a grant (5 MO1 RR00071) for the Mount Sinai General Clinical Research Center Program from the National Center of Research

Resources, a grant (5 P30 HD28822) for the Mount Sinai Child Health Research Center, and a research grant from the Genzyme Corporation. Many thanks to the Genzyme Pathology Department staff for their help in developing a histologic grading system, to the Medical Information Department for their help with extensive literature searches on Fabry Disease, and to Biometrics for statistical data analysis. We also thank the clinical investigators and their patients at the multiple sites who participated in this trial: C.M. Eng, M. Banikazemi, J. Ibraham, and A.P. Cheng (*New York, NY, USA*); W.R. Wilcox and L.J. Raffel (*Los Angeles, CA, USA*); N. Guffon and P. Cochat (*Lyon, France*); D.P. Germain, M. Azizi, and X. Jeunemaitre (*Paris, France*); P. Lee and A. Vellodi (*London, UK*); S. Waldek and J.E. Wraith (*Manchester, UK*); L. Caplan, C.J. Chaves, K.B. Kanis, I. Linfante, and R. Llinas (*Boston, MA, USA*); and C.E.M. Hollak, G.E. Linthorst, D.K. Bosman, H.S.A. Heymans, and F.A. Wijburg (*Amsterdam, The Netherlands*).

Reprint requests to Dr. Michael O'Callaghan, Department of Preclinical Biology, Genzyme Corporation, P.O. Box 9322, One Mountain Road, Framingham, Massachusetts 01701-9322, USA.
E-mail: mike.ocallaghan@genzyme.com

REFERENCES

1. Gubler MC, Lenoir G, Grunfeld JP, *et al*: Early renal changes in hemizygous and heterozygous patients with Fabry's disease. *Kidney Int* 13:223–235, 1978
2. Farge D, Nadler S, Wolfe LS, *et al*: Diagnostic value of kidney biopsy in heterozygous Fabry's disease. *Arch Pathol Lab Med* 109: 85–88, 1985
3. Marguery MC, Giordano F, Parant M, *et al*: Fabry's disease: Heterozygous form of different expression in two monozygous twin sisters. *Dermatology* 187:9–15, 1993
4. Desnick RJ, Ionnou YA, Eng CM: α-Galactosidase A deficiency: Fabry disease, in *The Metabolic and Molecular Bases of Inherited Disease* (8th ed, vol 3), edited by Scriver CR, Beaudet AL, Sly WS, Valle D, New York, McGraw-Hill, pp 3733–3774, 2001
5. von Scheidt W, Eng CM, Fitzmaurice TF, *et al*: An atypical variant of Fabry's disease with manifestations confined to the myocardium. *N Engl J Med* 324:395–399, 1991
6. Nakao S, Takenaka T, Maeda M, *et al*: An atypical variant of Fabry's disease in men with left ventricular hypertrophy. *N Engl J Med* 333:288–293, 1995
7. Colombi A, Kostyal A, Bracher R, *et al*: Angiokeratoma corporis diffusum-Fabry's disease. *Helv Med Acta* 34:67–83, 1967
8. Wallace HJ: Anderson-Fabry disease. *Br J Dermatol* 88:1–23, 1973
9. Eng CM, Banikazemi M, Gordon RE, *et al*: A Phase 1/2 Clinical Trial of enzyme replacement in Fabry disease: Pharmacokinetic, substrate clearance, and safety studies. *Am J Hum Genet* 68:711–722, 2001
10. Eng CM, Guffon N, Wilcox WR, *et al*: Safety and efficacy of recombinant human α-galactosidase: A replacement therapy in Fabry's disease. *N Engl J Med* 345:9–16, 2001
11. Sakuraba H, Igarashi T, Shibata T, Suzuki Y: Effect of vitamin E and ticlopidine on platelet aggregation in Fabry's disease. *Clin Genet* 31:349–354, 1987
12. Sterzel RB, Lovett DH: Interactions of inflammatory and glomerular cells in the response to glomerular injury, in *Immunopathology of Renal Disease. Contemporary Issues in Nephrology* (vol 18), edited by Wilson CB, Brenner BM, Stein JH, New York, Churchill Livingstone, 1988, pp 137–173
13. DeGraba T, Azhar S, Dignat-George F, *et al*: Profile of endothelial and leukocyte activation in Fabry patients. *Ann Neurol* 47:229–233, 2000
14. Savage CO: The biology of the glomerulus: Endothelial cells. *Kidney Int* 45:314–319, 1994
15. Stewart RJ, Marsden PA: Vascular endothelial cell activation in models of vascular and glomerular injury. *Kidney Int* 45(Suppl 45): S37–S44, 1994
16. Takano T, Brady HR: The endothelium in glomerular inflammation. *Curr Opin Nephrol Hypertens* 4:277–286, 1995
17. Nangaku M, Shankland SJ, Couser WG, Johnson RJ: A new model of renal microvascular injury. *Curr Opin Nephrol Hypertens* 7:457–462, 1998
18. Utsumi K, Yamamoto N, Kase R, *et al*: High incidence of thrombosis in Fabry's disease. *Intern Med* 36:327–329, 1997
19. Hulkova H, Ledvinova J, Poupetova H, *et al*: Postmortem diagnosis of Fabry disease in a female heterozygote leading to the detection of undiagnosed manifest disease in the family. *Cas Lek Cesk* 138:660–664, 1999
20. Collins AB: Immunofluorescence, in *Diagnostic Immunopathology*, edited by Colvin RB, Bhan AK, McCluskey RT, New York, Raven Press, 1995, pp 699–710
21. Hille-Rehfeld A: Mannose-6-phosphate receptors in sorting and transport of lysosomal enzymes. *Biochim Biophys Acta* 1141:177–194, 1995
22. Braulke T: Type-2 IGF receptor: A multi-ligand binding protein. *Horm Metab Res* 31:242–246, 1999
23. Pabst R, Sterzel RB: Cell renewal of glomerular cell types in normal rat. An autoradiographic analysis. *Kidney Int* 24:626–631, 1983
24. Nadasdy T, Laszik Z, Blick KE, *et al*: Proliferative activity of intrinsic cell populations in the normal human kidney. *J Am Soc Nephrol* 4:2032–2039, 1994
25. Nagata M, Nakayama K, Terada Y, *et al*: Cell cycle regulation and differentiation in the human podocyte lineage. *Am J Pathol* 153:1511–1520, 1998
26. Mosnier JF, Degott C, Bedrossian J, *et al*: Recurrence of Fabry's disease in a renal allograft eleven year after successful renal transplantation. *Transplantation* 51:759–762, 1991
27. Gantenbain H, Bruder E, Burger HR, *et al*: Recurrence of Fabry's disease in a renal allograft 14 years after transplantation. *Nephrol Dial Transplant* 10:287–289, 1995
28. Malouf M, Kirkman H, Buchanan P: Ultrastructure changes in antenatal Fabry's disease. *Am J Pathol* 82:13a, 1976
29. Tsutsumi A, Sato M, Sata K, *et al*: Early prenatal diagnosis of inborn error of metabolism: A case report of a fetus affected with Fabry's disease. *Asia Oceania J Obst Gynaecol* 11:39–45, 1985
30. Soonpaa MH, Daud AI, Koh GY, *et al*: Potential approaches for myocardial regeneration. *Ann N Y Acad Sci* 752:446–454, 1995
31. Rodriguez FH Jr, Hoffmann EO, Ordinario AT Jr, Baliga M: Fabry's disease in a heterozygous woman. *Arch Pathol Lab Med* 109:89–91, 1985
32. Grünfeld JP, Le Porrier M, Droz D, *et al*: Renal transplantation in patients suffering from Fabry's disease. Kidney transplantation from an heterozygote subject to a subject without Fabry's disease. *Nouv Presse Med* 4:2081–2085, 1975
33. Grünfeld JP, Lidove O, Barbey F: Heterozygotes with Fabry's disease, in *Contributions in Nephrology* (vol 136), edited by Schieppati A, Daina E, Sessa A, Remuzzi G, Basel, Karger, 2001, pp 208–210
34. Kawamura O, Sakuraba H, Itoh K, *et al*: Subclinical Fabry's disease occurring in the context of IgA nephropathy. *Clin Nephrol* 47:71–75, 1997
35. Miyasaki K: Renal accumulation of glycosphingolipids. Report of a case and a review of literature. *Nephron* 14:456–465, 1975
36. Chen HC, Tsai JH, Lai YH, Guh JY: Renal changes in heterozygous Fabry's disease – A family study. *Am J Kidney Dis* 15:180–183, 1990
37. Sivaloganathan S: Fabry's disease—A rare cause of sudden death. *Med Sci Law* 32:263–266, 1992
38. Fukushima M, Tsuchiyama Y, Nakato T, *et al*: A female heterozygous patient with Fabry's disease with renal accumulation of trihexosylceramide detected with a monoclonal antibody. *Am J Kidney Dis* 26:952–955, 1995
39. Wuthrich RP, Weinreich T, Binswanger U, *et al*: Should living related kidney transplantation be considered for patients with renal failure due to Fabry's disease? *Nephrol Dial Transplant* 13: 2934–2936, 1998
40. Yoshitama T, Nakao S, Takenaka T, *et al*: Molecular genetic, biochemical, and clinical studies in three families with cardiac Fabry's disease. *Am J Cardiol* 87:71–75, 2001
41. Ikari Y, Kuwako K, Yamaguchi T: Fabry's disease with complete atrioventricular block: Histological evidence of involvement of the conduction system. *Br Heart J* 68:323–325, 1992
42. Elleder M, Bradova V, Smid F, *et al*: Cardiocyte storage and hypertrophy as a sole manifestation of Fabry's disease. Report on a case simulating hypertrophic non-obstructive cardiomyopathy. *Virchows Arch A Pathol Anat* 417:449–455, 1990